Properties of surface plasmons strongly coupled to excitons in an organic semiconductor near a metallic surface

C. Bonnand, J. Bellessa,* and J. C. Plenet
Laboratoire de Physique de la Matière Condensée et Nanostructures, CNRS UMR 5586, Université Claude Bernard Lyon I, F69622 Villeurbanne Cedex, France

(Received 11 January 2006; revised manuscript received 19 May 2006; published 23 June 2006)

The properties of organic semiconductor excitons in strong interaction with surface plasmons are described. For this purpose, a *J*-aggregated cyanine dye layer is deposited on a silver film and studied with reflectometry experiments. The dependence of the Rabi splitting with the square root of the dye layer absorption and the width inversion of the reflectometry lines at the resonance are observed. The experimental spectra are well fitted using a transfer matrix method with a complex index. The comparison between experiments and simulations for layers in different configurations is qualitatively related to the role of the plasmon polarization in the interaction with the aggregated dye chains. Finally, large Rabi splitting of 300 meV are observed for pure dye layers. Characteristic behavior of the large coupling and the effect of asymmetrical absorption line shape are analyzed.

DOI: 10.1103/PhysRevB.73.245330 PACS number(s): 78.66.Qn, 71.36.+c, 73.20.Mf, 78.55.Kz

I. INTRODUCTION

In the vicinity of conducting surfaces, the emitting properties of material are altered compared to the emission in free space. When the emitter is very close to the surface, the contribution of surface plasmon modes in the emission become predominant.[1] Lifetime modifications related to the emission through surface plasmons have been observed. An enhancement of two orders of magnitude of the radiative rate have been obtained.[2] These experiments were performed in the weak coupling regime. We have recently demonstrated that the strong coupling regime can be reached with surface plasmons.[3] In this regime the interaction plasmon-emitter becomes predominant compared to the damping in the system. The strong coupling leads to a characteristic anticrossing in the dispersion line, and to the formation of mixed exciton/plasmon states. The strong coupling with surface plasmons has been observed in plane[3] and also in engraved geometries[4] and the Rabi splitting characteristic of the strength of the coupling is several hundreds of meV.

The aim of this paper is to study the detailed properties of the plasmon exciton interaction in an organic semiconductor. The emitting material is composed of aggregated cyanine dyes which present a high oscillator strength.[5] We use a planar geometry with an attenuated total reflection technique to study the surface plasmon. This experimental method is well suited due to its flexibility and to the easy access to the different parameters of the interaction. We show some general behavior, shared with other systems in the strong coupling regime, like semiconductor microcavities which have been extensively studied in this regime,[6] and some particular features of surface plasmons like the effect of the polarization.

The first part of the paper is devoted to the description of the samples and of the experimental setup. In the second part, reflectometry spectra are described and fitted using a transfer matrix method with a complex index.[7] The oscillator strength is deduced from these calculations. In the third part, the dependence of the Rabi splitting with the absorption of the dye layer is studied. The polarization effect related to the interaction of the plasmon TM polarized and an anisotropic layer are addressed. The last part is devoted to systems with very large Rabi splitting. We show that characteristic features of a very large coupling can explain the very asymmetric shape of the spectra at the resonance.

II. SAMPLES AND EXPERIMENTAL SETUP

The aggregated cyanine dyes present a large oscillator strength and are well suited for the observation of strong coupling.[6,8] We have used a cyanine dye: the 5,5′, 6,6′-tetrachloro-1,1′-diethyl-3,3′-di(4-sulfobuthyl)-benzimidazolocarbocyanine (TDBC), the developed chemical formula is given in inset of Fig. 1. Figure 1(a) presents the monomer absorption band of TDBC in water with a concentration of 10^{-5} mol L^{-1}. The spectrum is characterized by a large and asymmetric band at 2410 meV. When the concentration of TDBC in water increases, the dye molecules self-organize to form chains namely *J*-aggregates.[9] This new ordering of the dye molecules creates a delocalization of the

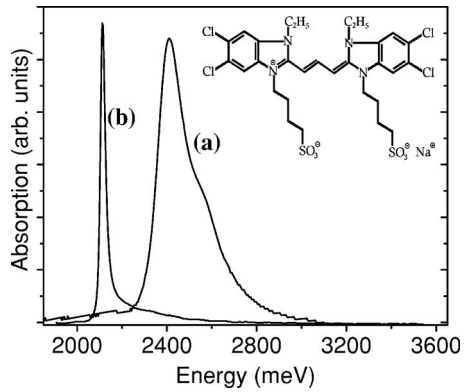

FIG. 1. Absorption spectra of TDBC monomer in water solution (10^{-5} mol L^{-1}) and of TDBC *J*-aggregates in water solution (10^{-3} mol L^{-1}). The inset shows the chemical formula of TDBC.

excitation which induces a redshift and a narrowing of the absorption band.[9] Figure 1(b) shows the *J*-band of TDBC in water with a concentration of 10^{-3} mol L^{-1}. The *J*-aggregate absorption spectrum is characterized by a single, narrow, and intense band lying at 2100 meV.

The experiments were performed on samples formed by a silver layer surrounded by an active layer containing the organic dye. A 50 nm thick silver film was fabricated by thermal evaporation under a pressure of 10^{-7} Torr on a pyrex glass substrate. A thin film of TiO_2 was deposited on silver by dip coating using the sol gel method.[10] This layer improves the adhesion of the organic layer. Two types of organic layers have been used in our experiments: pure TDBC layers and TDBC included in a polyvinilalcohol (PVA) matrix. In both cases, the layer is deposited by spin coating on the TiO_2 layer. For pure TDBC, the TiO_2 film thickness is around 15 nm, this thickness has been chosen to shift the angle position of the surface plasmon dispersion relation in an adequate region. A solution of TDBC dissolved in water is then spin coated on the TiO_2 layer, the layer obtained is 20 nm thick. For TDBC in PVA, the TiO_2 film is extremely thin (2 nm) and the dye is dissolved with various concentrations in a solution of PVA in water. The resulting solution is also deposed by spin coating, and formed a 30 nm thick layer.

To study the interaction between surface plasmon and the TDBC exciton, we have performed reflectometry experiments in the Kretschmann configuration.[11] The sample is positioned on an hemispherical prism (optical index 1.516 at 632.8 nm) on the glass side with glycerol (optical index 1.474 at 632.8 nm) to ensure the optical index continuity between the prism and the pyrex substrate. The hemispherical prism with the sample is mounted on a rotating holder. A TM-polarized monochromatic beam is focalized through the prism, on the center of the hemisphere. After reflection the beam is detected, the angle of detection is reduced by a slit which corresponds to a precision on the detection angle of 0.4°. We have recorded the intensity reflected by the sample as a function of the wavelength of the incident light, for a given angle.

III. EXPERIMENTS

Figure 2 shows the room temperature reflection spectra of a layer of PVA-TDBC on silver measured in the configuration described above, for different detection angles. Two dips are present in each spectrum. The dips correspond to exciton/plasmon mixed states: polaritons.[3,12] The energy separation between the two dips changes and has a minimum value of 150 meV at $\theta=51°$. The spectra have been recorded in TM polarization which corresponds to the polarization of surface plasmons. In TE polarization, the dips in the reflection spectra do not appear.

The reflectometry spectra are fitted using a conventional matrix method.[13] To take into account the optical characteristics of the TDBC in the layer, the dielectric constant of the active layer $\varepsilon_{layer}(e)$ is termed as (Ref. 14) follows:

$$\varepsilon_{layer}(e) = \varepsilon_{PVA}(e) + \frac{fq^2\hbar^2}{m\varepsilon_0 L_z}\frac{1}{e_0^2 - e^2 - i\gamma_0 e}, \qquad (1)$$

where ε_{PVA} is the dielectric constant of the PVA, e is the energy, f is the oscillator strength of the *J*-aggregate, γ_0 is the exciton linewidth, q the electron charge magnitude, m the electron mass, ε_0 the permittivity of the free space, and L_z the thickness of the layer. The optical indexes of the PVA layer and of the TiO_2 layer have been deduced from ellipsometry experiments and the one of the silver layer has been obtained in the literature.[15] The thickness of the PVA layer used is 26 nm and the energy ($e_0=2100$ meV) and width ($\gamma_0=49$ meV) of the exciton absorption in TDBC are deduced from absorption measurements on a layer deposed on a pyrex substrate without silver. The same parameters except the angle have been used for all fits. The calculated reflectometry spectra, presented in Fig. 2, are just rescaled, with the same constants for all spectra, to be comparable with the experimental spectra. The calculated spectra are in very good agreement with the experimental spectra. The oscillator strength deduced from the calculation is $1.8\times10^{14}\mathrm{cm}^{-2}$, this value is of the same order of magnitude as the oscillator strength found for this type of organic semiconductor in microcavities.[5]

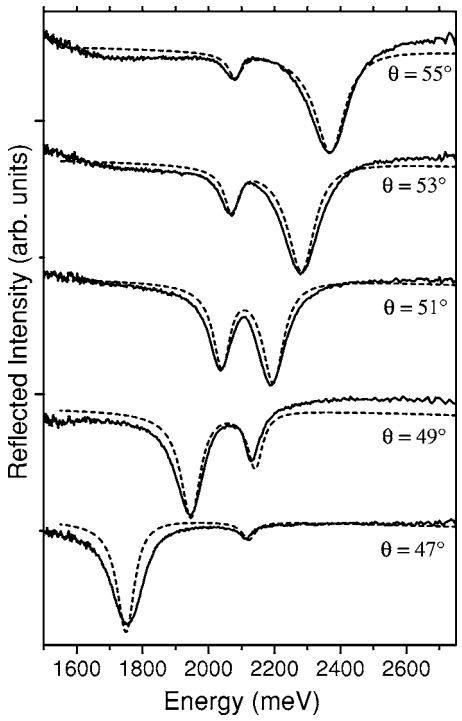

FIG. 2. Reflectometry spectra of a PVA-TDBC layer on silver for different detection angles as a function of the incident light energy. The dotted curves are calculated spectra using the transfer matrix method. The spectra are arbitrary translated for the clarity of the figure.

Figure 3(a) presents the energy of the reflectometry dips plotted as a function of the in-plane wave vector $k = \frac{2\pi n_p \sin(\theta)}{\lambda}$, where n_p is the index of the prism and θ the incident angle. A clear anticrossing between the two lines is present. The resonance occurs for $k=0.0125$ nm^{-1}, for this wave vector the energy separation between the two dispersion lines is minimal and has a value of 85 meV. This value is different from the minimal energy separation obtained in the reflectivity spectra of Fig. 2. This is related to the large energy separation of both dips of the spectrum recorded at

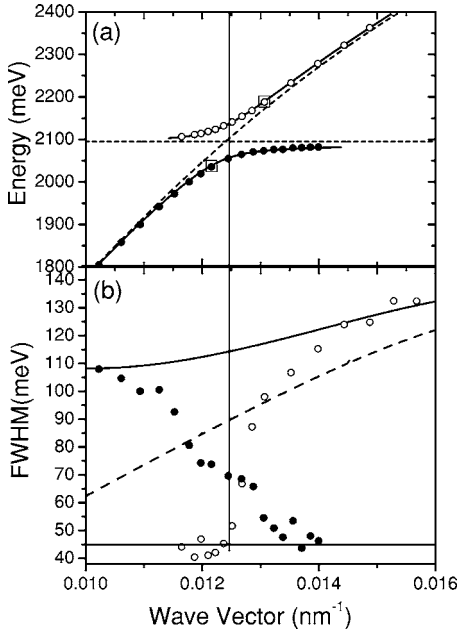

FIG. 3. (a) Presents the position in energy of each dip in the reflectometry spectra as a function of the wave vector. The dotted lines are the dispersion relations of an uncoupled surface plasmon and the TDBC exciton. From solid lines are drawn the calculated polariton energies. Both squares correspond to the reflectometry dips recording at $\theta=51°$. (b) Presents the linewidths of each dip as a function of the wave vector. The dashed line is the calculated width, and the upper solid line represents the calculated width taking into account the angular resolution of the experimental setup. The lower solid line is the width of the uncoupled TDBC exciton.

$\theta=51°$. This separation induces a large shift of the dip wave vectors from the resonance wave vector, as shown in Fig. 3 where the 51° dips are shown as squares.

The energy positions deduced from the transfer matrix calculations are shown in Fig. 3(a) and are in good agreement with the experimental data. The two uncoupled modes, namely the TDBC *J*-aggregate exciton mode and the surface plasmon mode with a layer without TDBC, are also shown in dashed line in Fig. 3(a). The uncoupled plasmon dispersion line is obtained with a transfer matrix method for a PVA layer without TDBC. Far from the resonance the polariton dispersion lines are very close to the lines of the uncoupled surface plasmon and of the TDBC exciton.

Figure 3(b) shows the linewidth of the reflectivity dips as a function of the in-plane wave vector. These linewidths were deduced from the experimental spectra of Fig. 2 by fitting Lorentzian functions. A width inversion occurs, for $k=0.0126$ nm^{-1} which corresponds approximately to the resonance wave vector, both dips have the same width.

The widths are compared to the width of the uncoupled TDBC excitons and surface plasmons. The uncoupled surface plasmon width, deduced from transfer matrix calculations, is shown by the dashed line in Fig. 3(b). A quantity characteristic of the enlargement introduced by the experimental aperture (0.4°) of the detection has been added. This quantity is the surface plasmon energy modification introduced by an angle modification of 0.4°. The width calculated bound the experimental values which reach the calculated uncoupled values far from the resonance, when the energies are close to the uncoupled energies. The effect of the detection aperture explain the difference between the calculated spectra and the experiments in Fig. 2 for low detection angles.

IV. ABSORPTION DEPENDENCE AND POLARIZATION

The dependence of the Rabi splitting as a function of the absorption of the active layer is studied. We measured the splitting energies for different samples, varying the *J*-aggregate concentration in the PVA matrix. The thickness of the active layer must remain constant in the different samples. Indeed as the electric field associated with the surface plasmons decreases exponentially with the distance to the interface, a layer thickness modification would modify the interaction. The thickness of the TDBC in the PVA layer has been checked with the angular position of the resonances. The lower concentration limit for the TDBC in PVA was the apparition of the strong coupling, and the upper limit was fixed by modifications of the resonance angular positions due to thickness or structural modifications of the PVA layer induced by the TDBC concentration. The ratio between the TDBC monomer and the PVA monomer ranges from 1.2×10^{-4} to 7.3×10^{-4}. For a larger TDBC concentration, the thickness of the layer increases (for the same deposition parameters) and the shape of the absorption line is modified.

The Rabi splitting measured are plotted in Fig. 5 as a function of the square root of the absorption. This absorption has been measured on a PVA+TDBC layer deposed on a glass substrate without a silver layer fabricated in the same condition as the layer deposed on a silver film. Figure 5 shows a linear dependence of the splitting with the absorption square root. This dependence is characteristic of systems in the strong coupling regime and has also been observed in optical microcavities.[16,5,17]

Each series of reflectometry spectra in the strong coupling regime has been fitted with a transfer matrix method. A complex dielectric constant, given by Eq. (1), has been used for the PVA-TDBC layer. Only the oscillator strength f changes from one sample to the other, the energy position e_0, the width γ_0, and the thickness of the layer used in the simulations remain constant. With the same dielectric constant, the absorption of the polymer layer deposed directly on a glass substrate has been calculated and compared to the experimental absorption spectrum. Both spectra for the same TDBC concentration are shown in Fig. 4. The calculated spectrum has the same position and shape as the experimental spectrum. But its intensity is 1.8 times lower than the experimental one. The ratio between the calculated and the measured absorption is the same for all the concentrations (with a precision of more or less 10%). The Rabi splitting as a function of the calculated absorption is shown in Fig. 5 and has a linear dependence in the same way as the Rabi splitting plotted as a function of the experimental dependence, but with a larger rate.

The difference between the calculated and the experimental absorption is the signature of polarization effects. The

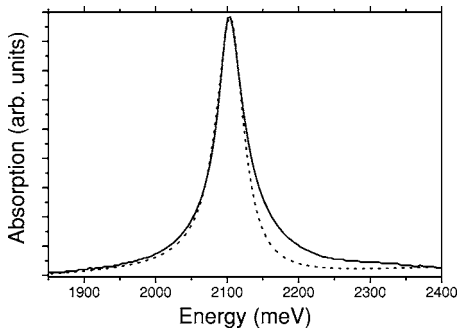

FIG. 4. Absorption spectrum of a layer of PVA-TDBC directly deposited on the substrate. The dashed line is the calculated absorption multiplied by a factor 1.80.

calculation corresponds to an isotropic absorbing layer and the real dye layer is anisotropic. Indeed, the TDBC monomers aggregate and form linear chains spread in the PVA matrix. Due to the thinness of the deposited layer, we can suppose that the chains and their dipole moment are mainly elongated in the plane of the layer. This anisotropic structure interacts with surface plasmons which propagate in the plane of the layer and are TM polarized. The plasmon electric field is mainly transverse, quasiperpendicular to the layer and to their dipole moment, the electric field is tilted by 20° from the normal to the interface. The absorption of the uncoupled TDBC is measured with an incidence normal to the surface, in this case the electric field is in the plane of the layers. The interaction between the light and the *J*-aggregate is more favorable when the electric field is in the plane of the layer which corresponds to the main direction of elongation of the dye chains compared to the case of surface plasmons with an electric field quasiperpendicular to the plane of the film. The difference between the calculated and the measured absorption results from the polarization of the surface plasmon and from the anisotropy of the *J*-aggregated dye layer.

V. VERY STRONG COUPLING

The final point of this paper deals with large Rabi splitting. In order to obtain the greatest coupling, we use samples containing pure TDBC layers. Figure 6 presents the absorption spectrum of such a film, deposited on a glass substrate. The shape of the absorption line is modified compared to the one of TDBC in a PVA matrix. A high energy tail appears, without any change to the linewidth and to the energy position of the peak.

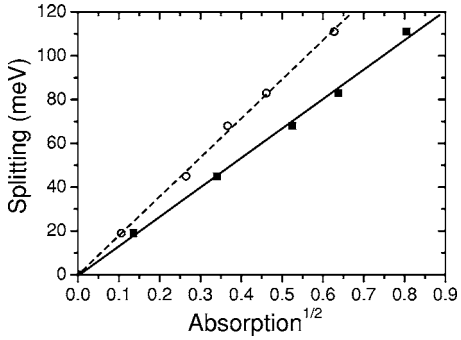

FIG. 5. In full squares are drawn the experimental Rabi splitting values as a function of the square root of the experimental absorption of the PVA-TDBC layer, in empty circles the Rabi splitting as a function of the square root of the calculated absorption.

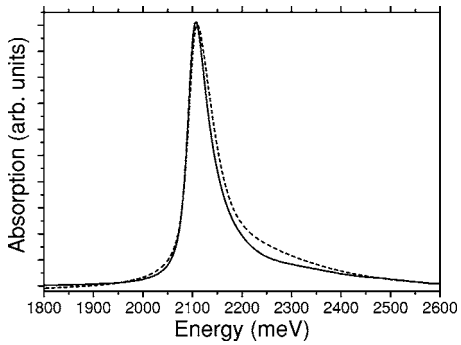

FIG. 6. The solid line presents the experimental absorption spectrum of a pure TDBC layer, the dashed line presents the calculated values.

Figure 7 shows a reflectometry spectrum of a sample made of pure TDBC on a silver layer in a Kretschmann geometry. The detection angle is 48° and corresponds to the minimal energy separation between both reflectometry dips. The energy separation is 700 meV. The reflectometry spectrum presents several differences compared to the equivalent spectrum of Fig. 2 (θ=51°). The width of both dips are very different and the low energy dip is deeper than the other. In Fig. 8 are presented the position and width of the dips as a function of the wave vector. The Rabi splitting obtained is 300 meV. Figure 8(b) shows that the dip width plotted as a function of the wave vector at the resonance are quasiequal. The difference in width between both dips at 48° is related to their large energy separation. In this case the positions of the dips do not correspond to the same wave vector, as described above for the dip separation energy.

Another effect has to be taken into account to explain the difference of deepness between both peaks in Fig. 7, which does not appear for TDBC in a PVA matrix (θ=51° of Fig. 2). This difference can be attributed to the presence of a high energy tail in the absorption of pure TDBC. To evaluate the

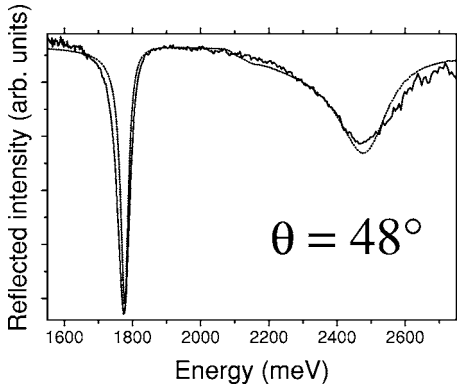

FIG. 7. Reflectometry spectrum of a pure TDBC layer on silver for an angle of detection of 48° as a function of the incident light energy. The dotted curve is the calculated spectrum.

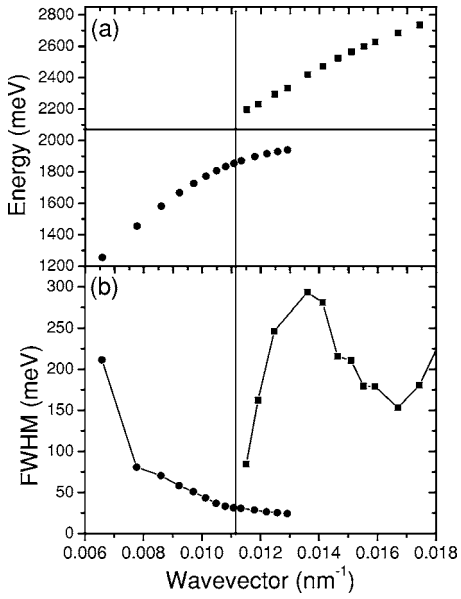

FIG. 8. (a) Presents the position in energy of each dip in the reflectometry spectra for pure TDBC layer on silver as a function of the wave vector. (b) Presents the linewidths of each dip as a function of the wave vector. The lines are guides for the eyes.

importance of this asymmetry of the absorption shape, we have fitted the reflectometry spectrum with the same conventional matrix method, using a dielectric constant which takes into account the asymmetry of the absorption spectrum. The imaginary part of the dielectric constant is the product of a Lorentzian function by a sum of three asymmetric functions $k(e)$ termed as, follows:

$$k(e) = \frac{1}{1+\exp\left(-\frac{e-e_0}{w_1}\right)}\left(1-\frac{1}{1+\exp\left(-\frac{e-e_0}{w_2}\right)}\right), \quad (2)$$

where e is the energy. All the functions of $k(e)$ are centered at the same energy $e_0=2100$ meV and have different parameters w_i. We have found the real part using the Kramers-Kronig relations. The parameters w_i in Eq. (2) are determined by fitting the absorption spectrum of a pure TDBC layer deposited directly on a pyrex substrate. The calculated absorption is shown in Fig. 6. The same complex index with the same shape is used for the calculation of reflectometry spectrum in the Kretschmann geometry. Calculated spectra are plotted as the dotted line in Fig. 7, there is a good agreement between the simulated and the experimental spectra. The dissymmetry in the line shape of the reflection spectra is due to the dissymmetry in the absorption spectra[18] and a very weak high energy tail modify the reflection spectra, similar results have been observed in microcavities.[19] Despite the difference of structure and thickness between pure TDBC layers and TDBC in PVA matrix, a similar ratio between the amplitudes of calculated and measured absorptions is obtained: 1.7 for pure TDBC layer compared to 1.8 for PVA +TDBC layers.

VI. CONCLUSION

In conclusion, a detailed study of the plasmon-exciton interaction in the strong coupling regime is presented. The dependance of the Rabi splitting in the square root of the absorption has been evidenced. The experimental spectra are well fitted using the transfer matrix method with a complex index. The comparison of experiments and calculations in different detection configurations, reflectometry in the strong coupling regime, and transmission, is related to polarization effects: the TM polarized surface plasmon interacts with the anisotropic TDBC layer. Finally, Rabi splitting of 300 meV have been observed. The width of the reflectivity dips, for this large energy splitting, is analyzed and the influence of the asymmetry of the absorption line on the spectra shape is shown.

*Electronic address: bellessa@lpmcn.univ-lyon1.fr

[1] P. T. Worthing, R. M. Amos, and W. L. Barnes, Phys. Rev. A **59**, 865 (1999).
[2] A. Neogi, C. W. Lee, H. O. Everitt, T. Kuroda, A. Tackeuchi, and E. Yablonovitch, Phys. Rev. B **66**, 153305 (2002).
[3] J. Bellessa, C. Bonnand, J. C. Plenet, and J. Mugnier, Phys. Rev. Lett. **93**, 036404 (2004).
[4] W. L. Barnes, W. A. Murray, J. Dintinger, E. Devaux, and T. W. Ebbesen, Phys. Rev. Lett. **92**, 107401 (2002).
[5] D. G. Lidzey, D. D. C. Bradley, M. S. Skolnick, T. Virgili, S. Wlaker, and D. M. Whittaker, Nature (London) **395**, 53 (1998).
[6] M. S. Skolnick, T. A. Fisher, and D. M. Whittaker, Semicond. Sci. Technol. **13**, 645 (1998).
[7] Y. Zhu, D. J. Gauthier, S. E. Morin, Qilin Wu, H. J. Carmichael, and T. W. Mossberg, Phys. Rev. Lett. **64**, 2499 (1990).
[8] R. F. Oulton, N. Takada, J. Koe, P. N. Stravinou, and D. D. C. Bradley, Semicond. Sci. Technol. **18**, 419 (2003).
[9] See *J-Aggregates*, edited by T. Kobayashi (World Scientific, Singapore, 1996).
[10] J. C. Plenet, A. Brioude, E. Bernstein, F. Lequevre, J. Dumas, and J. Mugnier, Opt. Mater. **13**, 411 (2000).
[11] E. Kretschmann and A. Raether, Z. Naturforsch. A **23**, 2135 (1968).
[12] V. M. Agranovich, M. Litinskaia, and D. G. Lidzey, Phys. Rev. B **67**, 085311 (2003).
[13] M. Born and E. Wolf, *Principles of Optics*, 6th ed. (Pergamon Press, Oxford, 1980).
[14] R. Houdré, R. P. Stanley, U. Oesterle, M. Ilegems, and C. Weisbuch, Phys. Rev. B **49**, 16761 (1994).
[15] P. B. Johnson and R. W. Christy, Phys. Rev. B **6**, 4370 (1972).
[16] T. B. Norris, J.-K. Rhee, C.-Y. Sung, Y. Arakawa, M. Nishioka, and C. Weisbuch, Phys. Rev. B **50**, 14663 (1994).
[17] G. S. Agarwal, Phys. Rev. Lett. **53**, 1732 (1984).
[18] A. Armitage, D. G. Lidzey, D. D. C. Bradley, T. Virgili, M. S. Skolnick, and S. Wlaker, Synth. Met. **111-112**, 377 (2000).
[19] J. Bloch, T. Freixanet, J. Y. Marzin, V. Thierry-Mieg, and R. Planel, Appl. Phys. Lett. **73**, 1694 (1998).